References

[1] Cristal, E. G., and G. L. Matthaei, A technique for the design of multiplexers having contiguous channels, *IEEE Trans. on Microwave Theory and Techniques*, vol MTT-12, Jan 1964, pp 88–93.
[2] Wenzel, R. J., Exact design of TEM microwave network using quarter-wave lines, *ibid*, pp 94–111.
[3] Ragan, G. L., *Microwave Transmission Circuits*, MIT Rad Lab Series, New York: McGraw-Hill, vol 9, 1948, pp 708–9.
[4] Guillemin, E. A., *Synthesis of Passive Networks*, New York: John Wiley, 1957.
[5] Weinberg, L., *Network Analysis and Synthesis*, New York: McGraw-Hill, 1962.
[6] Weinberg, L., Network design by use of modern synthesis techniques and tables, *Proc. NEC*, vol 12, 1956, pp 704–817.
[7] Ozaki, H., and J. Ishii, Synthesis of transmission-line networks and the design of UHF filters, *IRE Trans. on Circuit Theory*, vol CT-3, Dec 1956, pp 325–336.
[8] Ozaki, H., and J. Ishii, Synthesis of a class of strip-line filters, *IRE Trans. on Circuit Theory*, vol CT-5, Jun 1958, pp 104–109.
[9] Grayzel, A. I., A synthesis procedure for transmission-line networks, *IRE Trans. on Circuit Theory*, vol CT-5, Sep 1958, pp 172–181.
[10] Schiffman, B. M., and G. L. Matthaei, Exact design of band-stop microwave filters, *IEEE Trans. on Microwave Theory and Techniques*, vol MTT—12, Jan 1964, pp 6–15.
[11] Richards, P. I., Resistor transmission-line circuits, *Proc. IRE*, vol 36, Feb 1948, pp 217–220.
[12] Horton, M. C., and R. J. Wenzel, Distributed filter design using exact techniques, *Microwaves*, Apr 1964, pp 16–21.
[13] Mager, H., The Chebyshev normalized low-pass 3 dB frequency —a bone from the technical graveyard? *IEEE Trans. on Circuit Theory (Correspondence)*, vol CT-10, Jun 1963, pp 287–288.

Operation of the Ferrite Junction Circulator

C. E. FAY FELLOW, IEEE, AND R. L. COMSTOCK MEMBER, IEEE

Abstract—**The operation of symmetrical circulators is described in terms of the counter-rotating normal modes (fields varying as exp $n\phi$) of the ferrite-loaded circuits. The rotating modes, which are split by the applied magnetic field, form a stationary pattern which can be rotated in space to isolate one of the ports of the circulator. A detailed field theory of the strip-line *Y*-junction circulator operating with $n=1$ is presented. Experiments designed to confirm the validity of the rotating normal mode description of circulator action in the *Y*-junction circulator also are presented; these include measurements of mode frequencies and electric field patterns. The results of the field theory are used in a design procedure for quarter-wave coupled strip-line circulators. The results of the design procedure are shown to compare adequately with experimental circulators. Higher mode operation of strip-line circulators is described. The operation of waveguide cavity circulators is shown to depend on the rotating ferrite-loaded cavity modes.**

Introduction

A VERSATILE MICROWAVE DEVICE which is becoming one of the most widely used is the ferrite junction circulator. Its versatility is indicated by the fact that in addition to its use as a circulator, it also can be used as an isolator or as a switch. The three-port version of the ferrite junction circulator, usually called the *Y*-junction circulator, is most commonly used. It can be constructed in either rectangular waveguide or strip line. The waveguide version is usually an *H*-plane junction, although *E*-plane junction circulators also can be made. The strip-line ferrite junction circulator is usually made with coaxial connectors and is principally applicable to the UHF and low-microwave frequencies.

Manuscript received July 13, 1964; revised September 8, 1964.
C. E. Fay is with Bell Telephone Labs., Inc., Murray Hill, N. J.
R. L. Comstock is with Lockheed Missiles and Space Co., Research Labs., Palo Alto, Calif., He was formerly with Bell Telephone Labs., Inc., Murray Hill, N. J.

The ferrite junction circulator was in use for a number of years before its theory of operation received much attention in the literature. Early experimenters found that waveguide *T* junctions having a transversely magnetized ferrite slab suitably placed in the junction could, with proper matching and adjustment of the magnetic field, be changed into circulators. The bandwidth of such devices was very narrow. Refinements producing greater symmetry were found to increase bandwidth so that useful devices were obtained [1]–[4].

More recently a number of papers have appeared in the literature which bear on the theory of operation of the ferrite junction circulator. Auld [5] has considered the theory of symmetrical junction circulators in terms of the scattering matrix of the device. He has shown the necessary relations of the eigenvectors of the matrix, and has indicated how these relations may be obtained. Milano, Saunders, and Davis [6] have applied these concepts in the design of a *Y*-junction strip-line circulator. Bosma [7], [8], has made an analysis of the strip-line *Y*-junction circulator in terms of the normal modes of the center disk structure. In his second paper, he shows that the circulation condition is near a degeneracy of a pair of resonances of the disk structure. Butterweck [9] has considered the case of the waveguide junction circulator and has given the waveguide equivalent of Bosma's explanation. Others have attempted explanations based on field displacement, scattering from a post, or surface waves. All of these, if used with proper boundary conditions, conceivably could lead to the same conclusions.

This treatment will consist of an extension of Bosma's approach to the problem. First, we shall present a phenomenological description of the operation of the

strip-line Y-junction circulator followed by a development of the field theory applicable to this form of circulator, and then some experimental evidence of the validity of the approach will be submitted. Then, the theory is applied to provide a detailed design procedure for quarter-wave coupled strip-line circulators. Finally, we shall discuss operation in higher modes, operation of a four-port junction, and operation in rectangular waveguide.

I. Phenomenological Description

The strip-line Y-junction ferrite circulator consisting of two ferrite cylinders filling the space between a metallic conducting center disk and two conducting ground plates presents the simplest geometrical arrangement and, therefore, is the easiest to treat analytically. We shall present a development of the strip-line Y-circulator starting from more familiar concepts. This circulator in its basic form is illustrated in Fig. 1. The connections to the center disk are in the form of three strip-line center conductors attached to the disk at points 120° apart around its circumference. A magnetizing field is applied parallel to the axis of the ferrite cylinders.

It was found, experimentally, that the Y-circulator had some but not all of the properties of a low-loss transmission cavity. At its resonant frequency, it was well matched but slightly undercoupled, and a standing wave existed in the structure. The maximum isolation occurred almost at the frequency at which the insertion loss was minimum. The isolation at the third port and the return loss from the input port correspond quite well as the frequency is changed. The above experimental evidence suggests a resonance of the center disk structure as being an essential feature of the operation of the circulator. The lowest frequency resonance of the circular disk structure of Fig. 1 is the dipolar mode in which the electric field vectors are perpendicular to the plane of the disk and the RF magnetic field vectors lie parallel to the plane of the disk. This mode, as excited at port 1, is illustrated in the unmagnetized case by the standing-wave pattern of Fig. 2(a). In the case of an isolated disk, the RF H lines would curve over the edge of the disk and continue back on the underside. With ferrite cylinders on each side of the disk, the bottom cylinder behaves as a mirror image of the top one, and the analysis of the device need only be concerned with one cylinder. Ports 2 and 3, if open-circuited, will see voltages which are 180° out of phase with the input voltage, and about half of the value of the input voltage. If the standing-wave pattern is rotated, as in Fig. 2(b), then port 3 is situated at the voltage null of the disk and the voltages at ports 1 and 2 are equal. The device is equivalent to a transmission cavity between ports 1 and 2, and port 3 is isolated. The standing-wave pattern of Fig. 2(b) in which all fields vary as $e^{j\omega t}$ can be generated by two counter-rotating field patterns of the same configuration. Each of these patterns would involve an

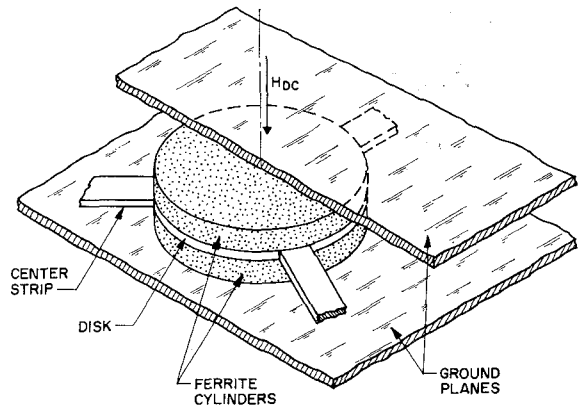

Fig. 1. Strip-line Y-junction circulator.

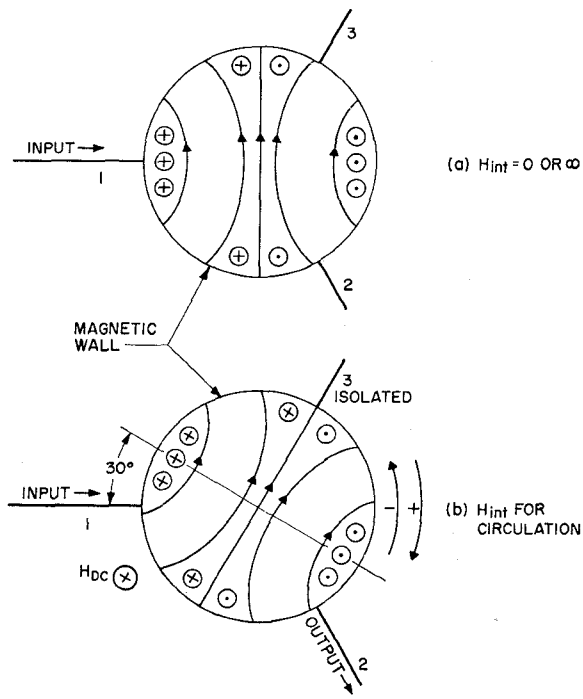

Fig. 2. (a) Dipolar mode of a dielectric disk. $H_{\text{int}}=0$ or ∞. (b) Analogous pattern of a magnetized disk. H_{int} for circulation. The pattern for the magnetized disk has been rotated to isolate port 3. The magnetic fields of higher modes than the dipolar mode are needed to achieve the pattern shown in (b).

RF magnetic field pattern which is circularly polarized at the center of the disk, becomes more elliptical as the radius increases, and is linearly polarized at the edge of the disk. If a magnetic biasing field (H_{dc}) is applied in the direction of the axis of the disk, the two counter-rotating patterns are no longer resonant at the same frequency. It is necessary when considering circulator action in the magnetized disk to include all of the normal modes, of which the dipolar field is but one, especially the nonrotating ϕ-independent mode ($n=0$ in the notation of Section II). This is the case since, as shown by Auld [5], circulator action must involve at least three normal modes. For the magnetized disk, the magnetic field pattern is a net pattern composed of many modes (the mode components of this pattern

will be derived under specialized assumptions in Section II). The pattern rotating, in the same sense as the electron spins of the ferrite cylinder tend to precess under the influence of the biasing field, will have an effective scalar permeability which we shall call μ^+ at the center of the cylinder, and an effective permeability μ_e for linear polarization at the edge of the disk. The pattern rotating in the opposite sense from the electron spin precession will have an effective scalar permeability μ^- at the center of the cylinder, and an effective permeability μ_e at the edge of the cylinder. Accordingly, we shall designate these split modes as "+" (plus) or "−" (minus) depending on their sense of rotation compared to that of the electron spin precession. If we excite the system of Fig. 2(b) at a frequency intermediate between the resonant frequencies of the split modes, the impedance of the + mode, which has the higher resonant frequency, will have an inductive reactance component, and that of the − mode, which has the lower resonant frequency, will have a capacitive reactance component. If the frequency chosen is such that the capacitive reactance component of one equals the inductive reactance component of the other, the total impedance will be real at the operating frequency f_0, Fig. 3. If the degree of splitting is adjusted such that the phase angles of the impedances of the two modes are each 30° ($|X/R| = \tan 30°$) at the operating frequency, then the standing-wave pattern will be rotated 30° from that which obtains with no splitting of the modes. This is illustrated in Fig. 2(b). The + mode, which has the inductive reactance component, will have its voltage maximum leading the current (or H-field) maximum at the input port by 30° in time phase, which is also 30° in space phase since for this mode there is one revolution per cycle. The − mode will have its voltage maximum lagging the current maximum at the input port by 30°. Therefore, the two voltage maxima will coincide at a point 30° away from the input port as shown in Fig. 2(b). The rotation of the *pattern* is in the direction of rotation of the + mode. This 30° rotation brings the E-field null of the pattern to port 3 so that no voltage exists at this port. However, for the power entering at port 1, the device acts as a transmission cavity with power leaving at port 2. Thus, the direction of circulation is the direction of rotation of the − mode for $H_{dc} < H_{res}$ (ferromagnetic resonance field); for $H_{dc} > H_{res}$, the circulation is in the opposite direction. Since the device has complete symmetry, any power entering at port 2 will set up a new set of similar modes which will result in this power leaving at port 3, and port 1 will be isolated. Similarly, power entering at port 3 is transmitted to port 1, and port 2 is isolated.

The sum of the impedances of the two counter-rotating modes gives the impedance of the stationary mode. This stationary resonance will have the same Q as each of its components, and will be the one to be considered when the loaded Q and the matching of the circulator are discussed. It is shown in the next section that the approximate equivalent circuit of the resulting stationary mode is a shunt resonator as indicated in Fig. 3.

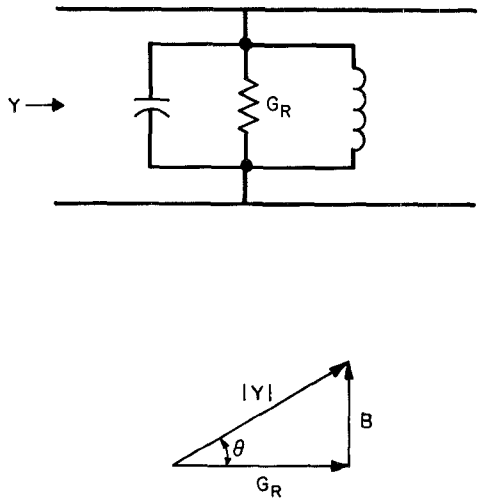

Fig. 3. Lumped element equivalent circuit of the stationary mode resonator.

We assume the resonator is lossless in this analysis so that the loaded Q, Q_L is described completely by the stored energy in the resonator and the power radiated into the connecting striplines. The field patterns of Fig. 2 are only those of the standing wave. The power transfer must be through a traveling wave whose fields are such as to result in an outgoing Poynting flux at port 2. In transmission cavities of large Q, the fields of the standing wave predominate. However, as Q_L becomes small this picture becomes inaccurate but still useful as will be shown by experimental results.

II. Field Theory of the Ferrite Junction Circulator

In the preceding section, a phenomenological description of circulator operation was presented. Here we will use the Maxwell equations, and the equations of motion of the magnetization to show the validity of the phenomenological picture and to arrive at some useful results relative to the design of this class of circulators. The boundary value problem which we shall discuss is the same as that considered by Bosma [7]. The circulator geometry consists of two ferrite cylinders separated by a disk center conductor fed by symmetrical transmission lines (see Fig. 1). The analysis is expected to predict the behavior of many similar circulators, e.g., the waveguide junction with a ferrite post.

Transverse electric (TE) waves with no variation along the dc bias field are considered. For these waves the electric field in the ferrite ($\boldsymbol{E} = \boldsymbol{a}_z E_z$) satisfies the homogeneous Helmholtz equation in cylindrical coordinates

$$\left[\frac{\partial^2}{\partial r^2} + \frac{1}{r}\frac{\partial}{\partial r} + \frac{1}{r^2}\frac{\partial^2}{\partial \phi^2} + k^2\right] E_z = 0 \qquad (1)$$

with time dependence $e^{j\omega t}$ and

$$k^2 = \omega^2\epsilon\epsilon_0\mu_{\text{eff}}\mu_0 = \omega^2\epsilon_0\epsilon\mu_0(\mu^2 - \kappa^2)/\mu \tag{2}$$

where μ and κ are the Polder tensor components appropriate to a normally magnetized disk [10]. Equation (1) has solutions, depending on the value of n, given by

$$E_{zn} = J_n(x)(a_{+n}e^{jn\phi} + a_{-n}e^{-jn\phi}) \tag{3}$$

where

$$x = kr$$

Maxwell's equations then give for the ϕ-component of $\vec{H}_n$

$$H_{\phi n} = jY_{\text{eff}}\left\{a_{+n}e^{jn\phi}\left[J_{n-1}(x) - \frac{nJ_n(x)}{x}\left(1 + \frac{\kappa}{\mu}\right)\right] + a_{-n}e^{-jn\phi}\left[J_{n-1}(x) - \frac{nJ_n(x)}{x}\left(1 - \frac{\kappa}{\mu}\right)\right]\right\} \tag{4}$$

with

$$Y_{\text{eff}} = \sqrt{\frac{\epsilon\epsilon_0}{\mu_0\mu_{\text{eff}}}}$$

As stated in the preceding section, it has been found useful to treat the circulator as a tightly coupled resonator. With this in mind, it is then of interest to find the character of the normal modes in the uncoupled case ($\psi = 0°$, where 2ψ is the angle subtended by the strip lines, Fig. 4). Even in the uncoupled case, it is difficult to record the exact boundary conditions. Bosma [8] has argued that the normal modes resulting from the boundary condition given by

$$H_\phi(r = R) = 0 \tag{5}$$

are sufficient for describing the field in the disk in the uncoupled case (Fig. 4 for $\psi = 0°$). Justification for this boundary condition is the exponential falloff of fields outside the disk boundary. The normal modes, which result when the boundary condition given by (5) is used with (4), have resonant frequencies given by the roots of

$$+ \text{ mode}, \quad J_{n-1}(kR) - \frac{nJ_n(kR)}{kR}\left(1 + \frac{\kappa}{\mu}\right) = 0$$

$$- \text{ mode}, \quad J_{n-1}(kR) - \frac{nJ_n(kR)}{kR}\left(1 - \frac{\kappa}{\mu}\right) = 0 \tag{6}$$

Several of the roots of these equations have been given by Bosma [8] in the form $(kR)_{m,n}^{\pm}$ vs. κ/μ, where m is the order of the root for a given value of n. For fixed value of m and n, there are two modes whose frequency separation depends on κ/μ and for small κ/μ is proportional to κ/μ. Fig. 5 shows a curve of κ/μ vs. σ where $\sigma = |\gamma| H_{\text{int}}/\omega$ with $p = |\gamma| 4\omega M_s/\omega$ as a parameter (H_{int} is the internal field and $4\pi M_s$ is the saturation induction). From an inspection of these curves, it is seen that $|\kappa/\mu|$ and hence the splitting is largest for a fixed value of p when $\sigma < 1$. This is shown, experimentally, to be the case in Section III. Also, it is evident that the splitting will vary rapidly with p (and hence $4\pi M_s$) in this region. The lowest root of (6) will be arrived at graphically after equations are derived relating to the coupled disk.

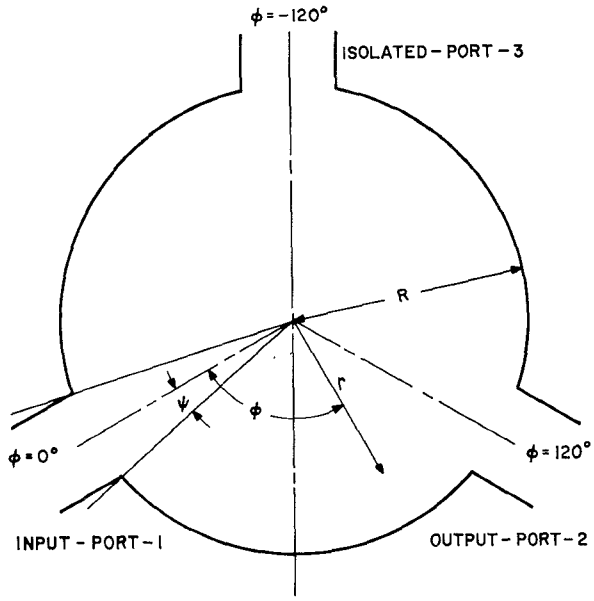

Fig. 4. Schematic diagram of strip-line circulator.

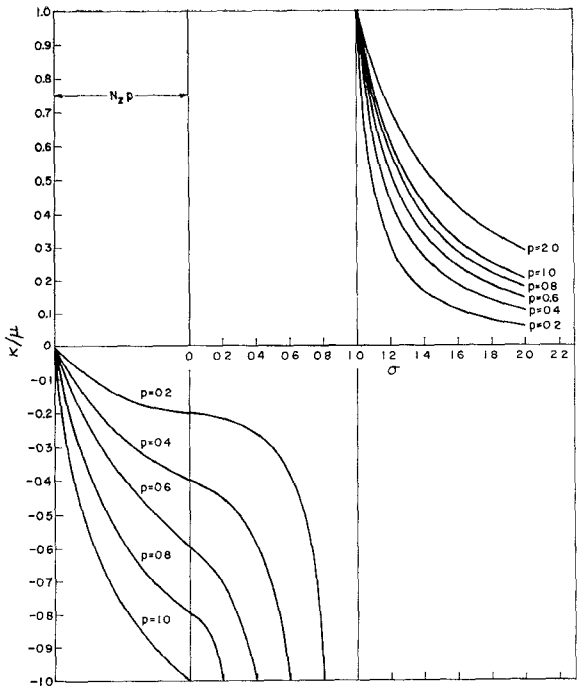

Fig. 5. κ/μ vs. σ, where $\sigma = |\gamma| H_{\text{int}}/\omega$.

The procedure we will use for treating the coupled case ($\psi \neq 0$), where the normal modes are driven by the TEM waves on the strip lines, is to assume initially that the system is functioning as a circulator and then to find the conditions on the rotating normal modes to satisfy the assumption. The conditions for circulator action are perhaps most easily described in terms of the

scattering matrix [5] but, in the field theory discussed here, it is necessary to state the conditions in terms of the electric and magnetic fields. We follow Bosma [7] in assuming H_ϕ to be constant over the width of the strip lines, and take for the boundary conditions at $r=R$

$$\left.\begin{aligned} -\psi < \phi < \psi, &\qquad H_\phi = H_1 \\ 120° - \psi < \phi < \psi + 120°, &\qquad H_\phi = H_1 \\ -120° - \psi < \phi < \psi - 120°, &\qquad H_\phi = 0 \\ \text{elsewhere}, &\qquad H_\phi = 0 \end{aligned}\right\} \tag{7}$$

and

$$\left.\begin{aligned} \phi = 0, &\qquad E_z = E_1 \\ \phi = 120°, &\qquad E_z = -E_1 \\ \phi = -120°, &\qquad E_z = 0 \end{aligned}\right\} \tag{8}$$

It is necessary for both E_z and H_ϕ to be zero at the isolated port ($\phi=-120°$) since the boundary condition there is an admittance boundary condition, i.e., the ratio of H_ϕ to E_z at this port must be the wave admittance.

To compute the complete function $E_z(\phi, R)$, it is assumed as an approximation that E_z has a sinusoidal distribution with one period around the periphery of the disk, i.e., only the $n=1$ mode is included for the electric field. The justification for this approximation is twofold: First, the amplitudes of the electric fields of the higher modes will be small since only the $n=1$ mode is near resonance; and second, measurements of the electric field described in Section III conform closely to such a sinusoidal distribution, at least for narrow-band circulators. Equation (3) with the boundary conditions (8) then gives for the mode amplitudes

$$a_+ = \frac{E_1}{2J_1(kR)}\left(1 + \frac{j}{\sqrt{3}}\right)$$

and

$$a_- = \frac{E_1}{2J_1(kR)}\left(1 - \frac{j}{\sqrt{3}}\right) \tag{9}$$

so that the total electric field is in the form of a sinusoidal standing wave

$$E_z = E_1 \frac{J_1(kr)}{J_1(kR)}\left(\cos\phi - \frac{\sin\phi}{\sqrt{3}}\right) \tag{10}$$

For the magnetic field, we expand the function specified in (7) into a Fourier series, as was done previously by Bosma [7], so that

$$H = H_1\left[\frac{2\psi}{\pi} + \sum_{n=1}^{\infty}\frac{\sin n\psi}{n\pi}\cos n\phi + \sqrt{3}\,\frac{\sin n\psi}{n\pi}\sin n\phi\right] \tag{11}$$

which for the $n=1$ mode can be written

$$H_{\phi_1} = H_1\frac{\sin\psi}{2\pi}\left[(1 - j\sqrt{3})e^{j\phi} + (1 + j\sqrt{3})e^{-j\phi}\right] \tag{12}$$

However, the $n=1$ component of H does not satisfy the circulation conditions. These conditions are satisfied only by the entire set of modes with the amplitudes given above.

Another solution for $H_{\phi 1}$ can be obtained from (4) by setting $n=1$ and using the values of the coefficients a_+ and a_- given in (9). The result

$$H_{\phi 1} = jY_{\text{eff}}\frac{E_1}{2J_1(kR)} \cdot \left\{\left(1 + \frac{j}{\sqrt{3}}\right)\left[J_0(kR) - \frac{J_1(kR)}{kR}\left(1 + \frac{\kappa}{\mu}\right)\right]e^{j\phi} + \left(1 - \frac{j}{\sqrt{3}}\right)\left[J_0(kR) - \frac{J_1(kR)}{kR}\left(1 - \frac{\kappa}{\mu}\right)\right]e^{-j\phi}\right\} \tag{13}$$

is only compatible with (12) if

$$J_0(kR) - \frac{J_1(kR)}{kR}\left(1 - \frac{\kappa}{\mu}\right) = -\left[J_0(kR) - \frac{J_1(kR)}{kR}\left(1 + \frac{\kappa}{\mu}\right)\right]$$

or

$$J_0(kR) = \frac{J_1(kR)}{kR} = 0 \tag{14}$$

of which the first root is

$$(kR)_{1,1} = 1.84 \tag{15}$$

This result is exact under the present boundary conditions and not approximate as assumed by Bosma [8]. By comparing (15) with the normal mode resonances in the uncoupled case (6), it is seen that $(kR)_{1,1}$ lies somewhere between $(kR)_{1,1}^+$ and $(kR)_{1,1}^-$. The exact value of operating frequency must be determined from a solution of (15) with k given by (2). In Fig. 6 is shown a graph of μ_{eff} vs. σ with p as a parameter for a thin disk. This curve is useful in conjunction with (15) in evaluating the disk radius R, given M_s, H_0, and ω. To illustrate the relationship of the operating frequency to the normal mode resonant frequencies, we show in Fig. 7 a plot of (6) ($n=1$) and (14) vs. kR.

One condition for circulation is that the operating frequency lie between the resonant frequencies for the $n=\pm 1$ modes. This is not the only condition since it is also required that the input admittance at port 1 and the output admittance at port 2 be adjusted to match the admittance at the terminals. Equating the values of H_{ϕ_1} given by (12) and (13), and taking account of the condition given by (14), leads to an expression for the input wave admittance of the circulator at resonance

$$Y_w = G_R = \frac{H_1}{E_1} \approx \frac{Y_{\text{eff}}\left|\,\kappa/\mu\,\right|}{\sin\psi} \tag{16}$$

which can be reduced to (69) of Bosma [7] for small ψ. The loaded Q of the circulator can be derived from the

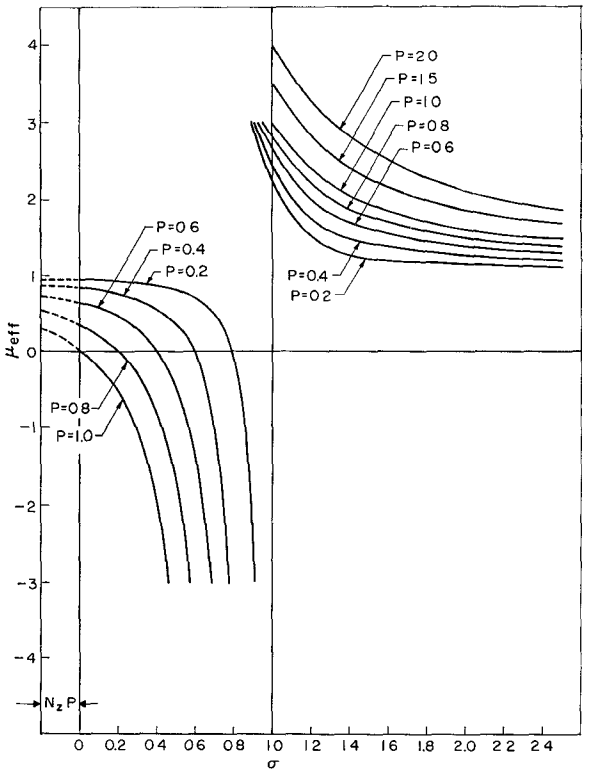

Fig. 6. μ_{eff} vs. σ

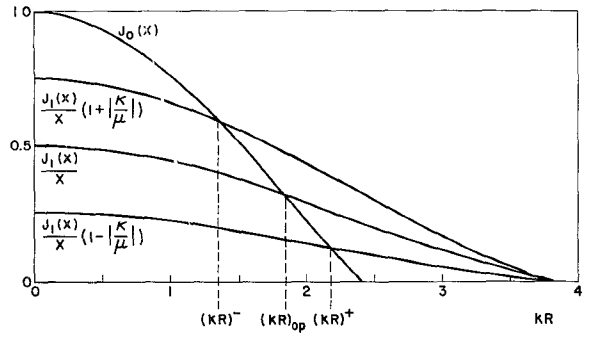

Fig. 7. Graphical solution of (9) and (17) for $n=1$. The operating frequency ($kR=1.84$) lies between the two normal mode resonances $(kR)^{\pm}$.

fields given in this section by starting from the definition

$$Q_L = \frac{\omega U}{P_{out}} \tag{17}$$

where U is the stored energy in the two cylinders and P_{out} is the power radiated out the strip lines. For U, we have

$$U = \frac{\epsilon\epsilon_0 d}{J_1^2(kR)} \int_0^{2\pi} \int_0^R E_m^2 J_1^2(kr) \cos^2 \phi' r dr d\phi'$$
$$= 1.11\, E_m R^2 d \epsilon\epsilon_0 \tag{18}$$

where E_m is the maximum electric field at the periphery of the disk, d is the cylinder height, and ϕ' has its zero reference at $\phi = -30°$. The total radiated output power is given by

$$P_{out} = d^2 E_m^2 G_R \cos^2 30° \tag{19}$$

where G_R is the conductance at the output strip lines and also the conductance looking into the resonator disk. Combining (17), (18), and (19), and evaluating the Bessel functions results in

$$Q_L = 1.48 \frac{\omega R^2 \epsilon\epsilon_0}{G_R d} \tag{20}$$

This result is physically satisfying because a large G_R is realized by making ψ large, which increases the coupling to the resonator.

It is possible to calculate the insertion loss of the ferrite cylinder and metallic disk circulator by calculating the unloaded Q, Q_0 of the structure as the result of including magnetic loss and dielectric loss. Since the expression for the resonant frequency and standing-wave pattern at the operating point involved only μ_{eff}, [(14) and (2)], if we assign a magnetic loss component to μ_{eff} so that

$$\mu_{eff} = \mu'_{eff} - j\mu''_{eff}$$

then the magnetic Q, Q_μ is just

$$\frac{\mu'_{eff}}{\mu''_{eff}}$$

From [11], we find

$$\mu_{eff} = \frac{1 - (p + \sigma + j\alpha)^2}{1 - (\sigma + j\alpha)(p + \sigma + j\alpha)} \tag{21}$$

where the loss has been introduced by substituting for σ, $\sigma + j\alpha$, where $\alpha = \gamma \Delta H / 2\omega$ is the resonance linewidth in the usual reduced units. Separating the real and imaginary parts of (21) we find, taking their ratio and neglecting terms in α^4, that

$$Q_\mu = \frac{\mu'_{eff}}{\mu''_{eff}}$$
$$= \frac{(p\sigma + \sigma^2 - 1)[(p+\sigma)^2 - 1] + \alpha^2(2\sigma^2 + 3\sigma p + p^2 + 2)}{\alpha p[(p+\sigma)^2 + 1]} \tag{22}$$

In the case of $\sigma = 0$, this expression reduces to

$$Q_\mu = \frac{1 - (\kappa/\mu)^2}{[1 + (\kappa/\mu)^2]\alpha\kappa/\mu} \tag{23}$$

For most circulators operated below resonance, p and κ/μ are $\ll 1$ and the unloaded Q can be approximated by

$$Q_\mu = \frac{2\omega^2}{\gamma^2 4\pi M_s \Delta H} \tag{24}$$

Likewise, the dielectric loss can be taken into account if we know the dielectric loss tangent of the ferrite. For this we have $Q_\epsilon = \epsilon'/\epsilon'' = 1/\tan\delta$. Then the total un-

loaded Q, Q_0 neglecting conductor losses is given by

$$\frac{1}{Q_0} = \frac{1}{Q_u} + \frac{1}{Q_\epsilon} \tag{25}$$

The insertion loss in dB is then, at band-center

$$\text{IL (dB)} = 10 \log_{10}\left(1 - \frac{Q_L}{Q_0}\right) \tag{26}$$

This represents a lower limit since the loss is assumed to be due to the fields of the standing wave only, and the conductor losses are not included.

The analysis up to this point has resulted in equations for the loaded Q of a single resonator. To relate the properties of this resonator to those of the two rotating normal modes, we express the electric field from (3) in terms of the normal mode fields, at $r=R$.

$$E_z = E^+ e^{-j\phi} + E^- e^{j\phi} \tag{27}$$

where, from (9)

$$E^\pm = \frac{E_1}{2}\left(1 \pm \frac{j}{\sqrt{3}}\right)$$

When both sides of (27) are divided by H_1, the driving magnetic field, and evaluated at $\phi=0$, we find expressions for the impedances for the two normal modes at port 1 at the operating frequency ω_{op}

$$Z^\pm = \frac{1}{2G_R}\left(1 \pm \frac{j}{\sqrt{3}}\right) \tag{28}$$

The input impedance is given by

$$Z = Z^+ + Z^- = \frac{1}{G_R} \tag{29}$$

These impedances can be represented by the lumped constant resonators shown in Fig. 8(a). The resonant frequencies of the resonators ($\omega^\pm$) are given by the roots of (6). The impedances of the + and − resonators at ω_{op} have phase angles of $\pm 30°$ as described in Section I. The operating frequency is approximately midway between the + and − mode resonant frequencies, i.e.,

$$\omega_{op} \approx \frac{\omega^+ + \omega^-}{2} \tag{30}$$

A detailed analysis of this equivalent circuit shows that in the vicinity of band-center, the two resonant circuits can be replaced by the single shunt resonator shown in Fig. 3 with the conductance on resonance and Q determined by (16) and (20).

Since the individual rotating mode resonators have 30° phase angles at band-center, a definite relation exists between the splitting $2\delta' = (\omega^+ - \omega^-)/\omega$, and the loaded Q, i.e.,

$$2\delta' = \frac{\tan 30°}{Q_L} = \frac{1}{\sqrt{3}Q_L} \tag{31}$$

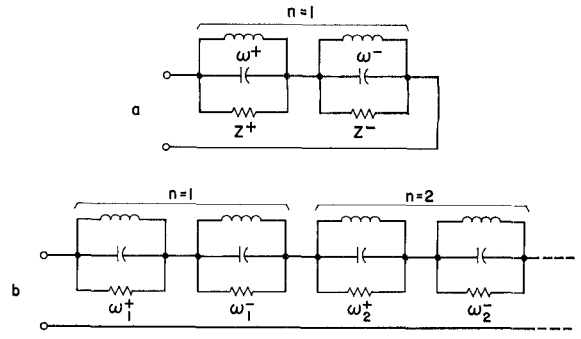

Fig. 8. Equivalent circuit of rotating normal modes ($\omega^\pm$). The $n=1$ mode resonances are shown in (a), and the more general circuit is shown in (b).

Equation (31) has been derived for the waveguide circulator by Butterweck [9] and is expected to be a general result for all three-port circulators which operate on the principle of the splitting of normal modes. A generalization of the above arguments for the higher order modes of the disk leads to the equivalent circuit shown in Fig. 8(b). In Sections III and IV it is shown that circulator action is possible between the resonances of the higher modes as represented in the equivalent circuit by the additional resonators. For example, if $\omega_{op} \approx (\omega_2^+ + \omega_2^-)/2$, the $n=1$ and all other modes are effectively short circuits, and we have the equivalent circuit similar to that shown in Fig. 8(a).

In Section IV, these results will be applied to the design of a stripline circulator. In the next section, some pertinent experimental results will be quoted.

III. Experimental

In this section, experimental evidence in support of the concepts developed in Sections I and II is presented. The experimental data have been taken on an L-band strip-line circulator which has dimensions large enough to allow probing of the electric fields at the edge of the center disk with sufficient mechanical accuracy so that relatively smooth plots are obtained.

A mode plot of the circulator is given in Fig. 9, which relates the mode resonances to the external field, H_{dc}. For the purposes of this plot, the center disk structure is lightly coupled to the 50-ohm strip lines by means of quarter-wave sections of high impedance line. This is done so that the various modes of the disk structure will be lightly loaded, and the resonances sharp and easily distinguished. The plot of resonant frequency as a function of applied magnetic field in Fig. 9 shows the $n=\pm 1$ modes, the $n=\pm 2$ modes, and parts of the $n=0$ and $n=+3$ modes. For circulator purposes, we are interested principally in the $n=1$ modes since these involve the smallest size of the disk structure for a given frequency and, therefore, presumably the least loss in the structure. The points of circulation are shown on the plot. These occur near the degeneracies of modes of like n. The sense of circulation, also indicated, is for the H_{dc} vector pointing toward the viewer. It will be noted that the sense of circulation for a given set of modes

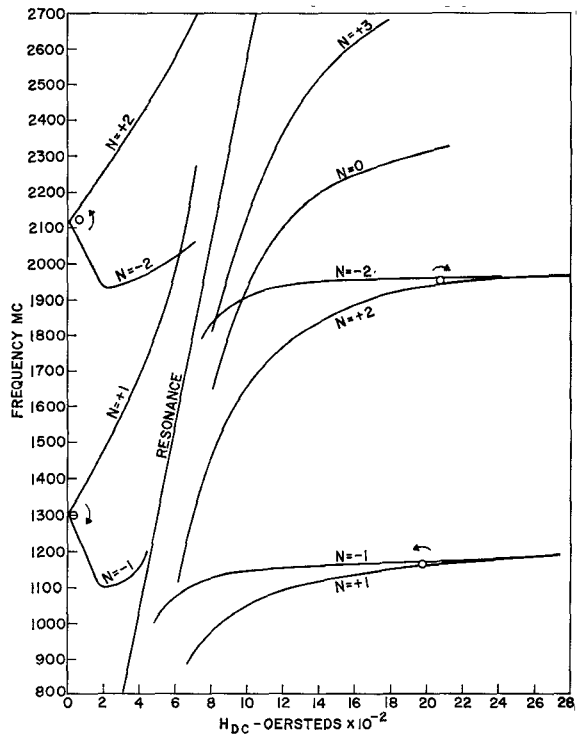

Fig. 9. Mode chart of experimental L-band circulator. Circulation is observed at the positions of the circles in the directions shown.

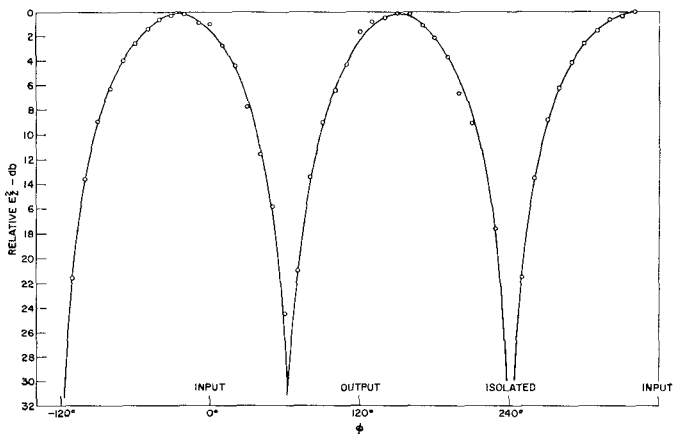

Fig. 10. Measured electric field at the periphery of a loosely coupled circulator. The measured curve is predicted accurately by the function 20 log (cos ϕ+sin ϕ/tan 120°).

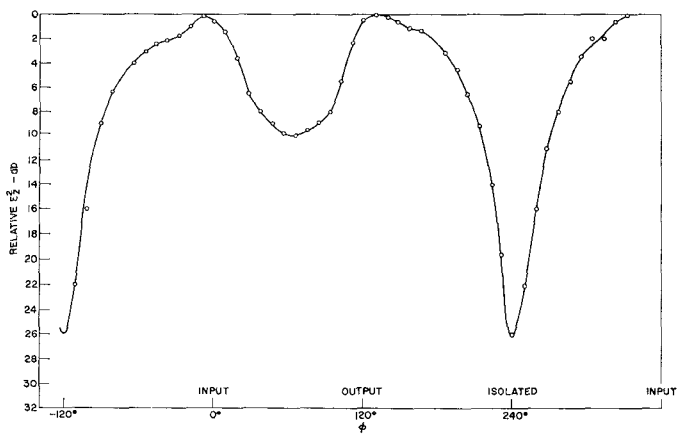

Fig. 11. Measured electric field at the periphery of a tightly coupled circulator.

above ferrimagnetic resonance is opposite to that for the same set of modes below ferrimagnetic resonance. The reason for this is that the − mode is the lower frequency one below resonance, and the higher frequency one above resonance. Therefore, the sign of the reactance of this mode at the operating frequency changes from the below resonance to the above resonance case, and hence, the sense of circulation will change if the reasoning given in Section I is followed. For the $n=2$ mode, the sense of circulation in each case is opposite to that of the corresponding $n=1$ mode case. The reason for this will be considered in the discussion of higher mode circulators.

A plot of the relative electric field, E_z, at the edge of the disk for the lightly coupled circulator is shown in Fig. 10. The circulator was adjusted for the below resonance point of circulation near the convergence of the $n=1$ modes, and the electric field probed at points around the circumference of the disk. The distribution is very nearly sinusoidal as predicted, with a slight distortion at the points where the high impedance feed lines are connected. The field maxima are seen to be approximately 30° away from the input and output ports. The circulator is very narrow-band in this case, and the required biasing field quite small, ~20 oersteds.

A more heavily coupled case is shown in Fig. 11. Here the same center structure is coupled to the 50 ohm strip lines by means of low impedance quarter-wave sections. This provides a more representative circulator which instead of being extremely narrow band, as in the previous case, has a >25 dB isolation bandwidth of approximately 15 per cent. The frequency of operation is nearly the same as before, but the required biasing field has increased to about 200 oersteds. This implies a greater separation or splitting of the modes as indicated in Fig. 9. The field plot of Fig. 11 shows a greater distortion in the vicinity of the connections to the center disk, as might be expected, since these connections are now considerably wider than in the previous case ($\psi=22°$). The other result to be noted is that the minimum in the electric field between the input and output ports is much shallower than previously. Aside from the distortions discussed above, it is obvious that the standing-wave pattern in this case is maintaining the 30° rotation predicted but is requiring a greater mode separation to do so. This greater mode separation is required in order to maintain the 30° admittance phase angles with the lower loaded Q of the modes which results from the heavier coupling to the strip lines.

IV. Y-Circulator Design Considerations

The design of a strip-line circulator employing the circular disk and ferrite cylinder form can be carried out using the principles discussed in Sections I and II.

The result will yield a reasonable approximation to the desired operating characteristics.

The use of the circulation condition between the resonances of the $n=1$ modes seems most desirable since this results in a minimum diameter of the metallic disk and ferrite cylinders. There seems to be no advantage in using the higher modes for a simple Y-circulator. The design will be based on the use of a quarter-wave transformer for coupling the circulator to the strip lines.

We must first choose the isolation bandwidth of the circulator. This is usually one of the things specified for the particular application of the circulator. Since the isolation of a Y-circulator usually corresponds quite closely to the return loss at the input port, and the return loss at the input port can be converted to VSWR (voltage standing-wave ratio), we define the following:

δ = fractional frequency deviation from f_0 (band-center) = $\frac{1}{2}$ bandwidth
VSWR = voltage standing-wave ratio at input port at frequencies $f=f_0(1\pm\delta)$
Y_R = admittance of disk resonator at $f=f_0(1\pm\delta)$
G_R = conductance of disk resonator
θ = phase angle of Y_R
Q_L = loaded Q of the disk resonator
δ' = fractional frequency splitting required for an admittance phase angle of 30° at the resonator

The resonator is assumed to have the equivalent circuit of Fig. 3. If a quarter-wave transformer or equivalent means is used for matching the resonator to the connecting strip lines, the susceptance of the transformer at $f=f_0(1\pm\delta)$ can be used to cancel that of the resonator at these frequencies. For these frequencies, it can then be shown that for small δ

$$\text{VSWR} \approx \frac{|Y_R|^2}{G_R^2} = \sec^2\theta \tag{32}$$

which allows us to determine θ. Then

$$Q_L = \frac{\tan\theta}{2\delta} \tag{33}$$

and we can find δ' from (31) using Q_L found previously. Since δ' relates to the amount of "splitting" required of the two $n=1$ modes, using (6), the value of κ/μ can be determined. Since the relation of δ' to κ/μ is approximately linear for small splitting, we find an approximate relation

$$\frac{\kappa}{\mu} = 2.46\delta' = \frac{0.71}{Q_L} \tag{34}$$

that is useful for design purposes. The value of the constant in the above equation is appropriate for values of κ/μ in the range 0.25 to 0.5 which should cover the most practical cases. Having found the value of κ/μ for the desired bandwidth, we find from Fig. 5 that we can obtain it with the biasing field in the ferrite either above or below that required for resonance, i.e., $\sigma>1$ for above resonance, or $\sigma<1$ for below resonance, where $\sigma=\gamma H_{\text{int}}/\omega$. Above resonance operation requires a somewhat smaller disk diameter, a higher saturation, p, where $p=\gamma 4\pi M_s/\omega$; and a higher biasing field, hence, a larger magnet. Below resonance operation requires a minimum field and a relatively low-saturation material, ($p<1$). Most Y-circulators in use at the present time employ the below resonance type of operation. For minimum field requirements it is convenient to operate at $\sigma=0$ which implies that the ferrite is just saturated or $H_{dc}\approx N_z 4\pi M_s$. From Fig. 5 and 6, it can be seen that at $\sigma=0$, $p=\kappa/\mu$ and $\mu_{\text{eff}}=1-(\kappa/\mu)^2$. It is now possible to calculate R, the disk radius, from (2) and (15) assuming the value of ϵ is known.

It is of course acceptable to use a lower value of p than that determined previously at the expense of increased biasing field. On the other hand, if too low a value of p is chosen, operation too close to $\sigma=1$ may be required and resonance losses will be appreciable. If higher values of p are used, the ferrite is operated below saturation, and hence, low-field loss may be experienced.

The remaining dimension to be found is the height of the ferrite cylinder, d. Equation (20) may be rewritten as

$$G_R d = \frac{1.48\omega R^2\epsilon\epsilon_0}{Q_L} \tag{35}$$

where everything on the right-hand side is already known. Thus, if we choose a value of G_R, the height d is determined. However, G_R cannot be specified until the matching is provided.

So far it has been assumed that a quarter-wave transformer will be used for matching and that its susceptance at the band edges will cancel the resonator susceptance at these points. In the admittance Smith chart of Fig. 12, there are shown two radii which represent the loci of admittances at $f_0(1+\delta)$ and $f_0(1-\delta)$ looking into a terminated transformer which is a quarter wavelength long at f_0, the band-center. Also shown are dotted curves representing loci of admittances having phase angles θ from (32). The example of Fig. 12 is taken for a bandwidth of 15 per cent ($\delta=0.075$) with 30 dB isolation (VSWR = 1.065, $\theta=14.3°$). The intersections of the radii and dotted loci define a resonator having the desired Q_L. The value of G_R and the characteristic admittance of the transformer, Y_T, now are determined if we specify the characteristic admittance, Y_0, of the strip line. Assuming for the example that $Y_0=0.02$ mho (50 ohm), then $Y_T=0.048$ mho and $G_R=0.115$ mho. The resonator admittance characteristic is seen to be wrapped into a tight loop at the end of the transformer and then transformed to a match at f_0, and to approximately the desired VSWR at the crossover point, $f_0(1\pm\delta)$.

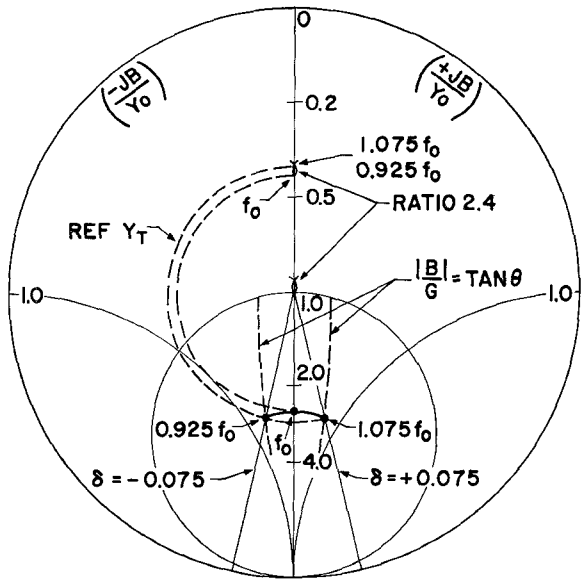

Fig. 12. Smith chart showing quarter-wavelength transformation to achieve a wide-band match. In this case the circulator is matched at midband with a 30 dB isolation bandwidth of 15 per cent.

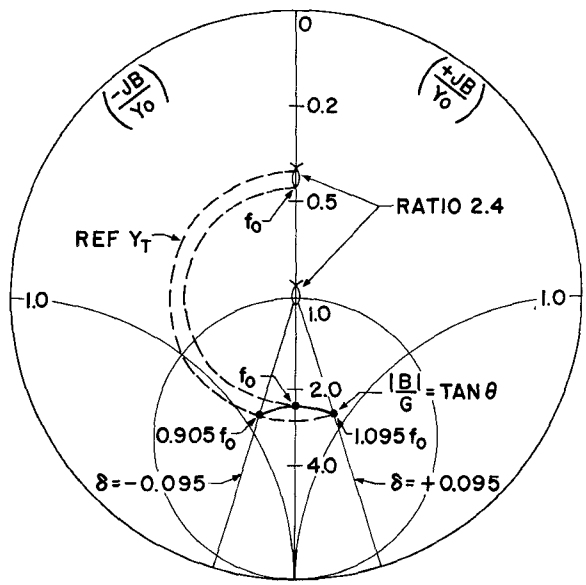

Fig. 13. Quarter-wavelength transformation for wide-band match with ripple in the isolation response. The 30 dB isolation bandwidth is 19 per cent in this case.

On inspection of Fig. 12, it will seem obvious that if either the transformer ratio or G_R of the resonator were changed slightly, the loop could be moved so that the origin was at its center, and the VSWR would be more uniform over the band. On the other hand, a larger loop could be used, still keeping all points within the specified VSWR. In Fig. 13, we show the latter case with the loop laid out so the midband point and the band edges all lie on a 1.065 VSWR circle. Using the same transformer ratio and working backward as compared to the previous procedure, it is found that G_R is now 0.108 mho and $\delta \approx 0.095$ with $\tan\theta = 0.310$, $Q_L = 1.63$. The value of G_R found in the foregoing can be used in (35) to find the thickness of the ferrite cylinder, d.

TABLE I
COMPARISON OF DESIGN AND ACTUAL CIRCULATORS

Design quantity	From fig. or eq.	L-Band Circulator		C-Band Circulator	
		19% B-W design	actual	19% B-W design	actual
Q_L	(33)	1.63	1.72	1.63	1.2
κ/μ	(34)	0.435	~0.5	0.435	~0.59
p	Fig. 5	0.435	0.52	0.435	0.28
μ_{eff}	Fig. 6	0.81	*	0.81	~0.6
ϵ		14	*	14	14
R cm	(15)	2.01	2.10*	0.655	0.76
$4\pi M_s$ gauss	$\frac{p\omega}{\gamma}$	200	240	625	400
G_R mho	Fig. 13	0.108	0.112	0.108	0.082
Y_T mho	Fig. 13	0.048	0.049	0.048	0.041
d cm	(35)	0.342	0.310	0.112	0.133
H_{dc} oers	$N_z 4\pi M_s$	145	~200	450	~870
Insertion loss dB	(26)	0.15	~0.1*	0.15	~0.17
30 dB Bandwidth	Fig. 13	0.19	0.185	0.19	0.12

* This structure has a 1.35-inch diam. ferrite cylinder inside a 1.75-inch-diam. alumina ring, hence μ_{eff} and ϵ will not be uniform and there is less material having magnetic loss than assumed in the design.

The result of the foregoing 19 per cent bandwidth design for 30 dB isolation compared to actual data on two circulators is shown in Table I.

Both circulators listed in the table were designed before the procedure outlined here was developed. The L-band circulator is observed to approximate fairly closely the design outlined.

V. Higher Mode Circulators and Other Forms

In this section we briefly sketch the operation of other strip-line circulators and also some waveguide circulators.

Y Circulator Using the $n=2$ Modes

As indicated previously, a Y circulator can be made using the $n=2$ modes (also $n=4$ and higher, excluding those having threefold symmetry). The resonator pattern rotation required for the $n=2$ mode is shown in Fig. 14. The required rotation in this case is 15° geometrically which corresponds to 30° electrically since this mode has two cycles around the circumference of the disk. The direction of rotation of the pattern is the same as the sense of circulation for this circulator.

The Four-Port Single Junction Circulator in Strip Line

The four-port single junction or X-junction circulator [12] seems attractive from the standpoint of compactness. An additional parameter is required [5] for this circulator as compared to the three-port junction. In this case, $n=1$ modes are split as in the three-port circulator and, in addition, the $n=0$ mode, which cannot split, is tuned to the operating frequency of the split $n=1$ modes. The resonator standing-wave patterns are illustrated in Fig. 15. The $n=1$ mode standing-wave pattern is rotated 45° toward the output port. With the

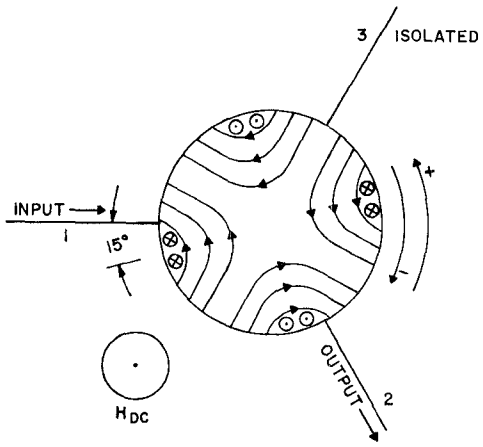

Fig. 14. Mode pattern for $n=2$ mode operation of disk circulator.

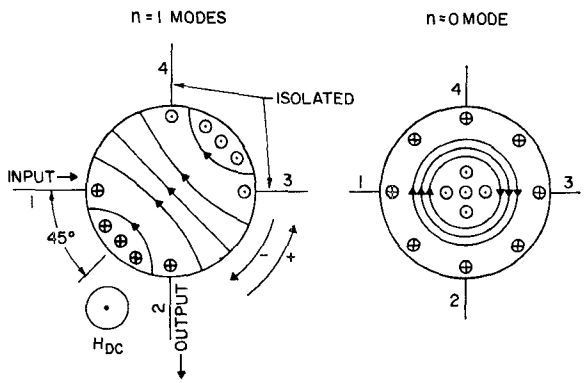

Fig. 15. Four-port circulator synthesized from $n=1$ and $n=0$ modes.

$n=0$ mode excited by the input port and with equal E-fields for the two patterns at the input port, the fields are also equal and in phase at the output, port 2. However, at ports 3 and 4, the fields are in opposite phase and will cancel. Thus we have transmission from port 1 to port 2, and ports 3 and 4 are isolated. The $n=0$ mode, which is normally about twice the frequency of the $n=1$ modes can be tuned lower in frequency by means of a capacitive post extending from the ground plane through a hole in the center of the ferrite cylinder to close proximity to the center of the metallic center disk. This post also raises the frequency of the $n=1$ modes somewhat so that the two resonant frequencies converge more rapidly. An $n=0$ mode of the cavity enclosing the ferrite strip-line assembly can be used in place of the $n=0$ disk mode. Therefore, this mode may be found to be more easily brought to the desired operating frequency.

The Y-Junction Circulator in Rectangular Waveguide—The H-Plane Junction

The three-port waveguide circulator usually consists of a 120° H-plane junction having a post of ferrite at the center of the junction as shown in Fig. 16. The biasing magnetic field is applied in the direction of the

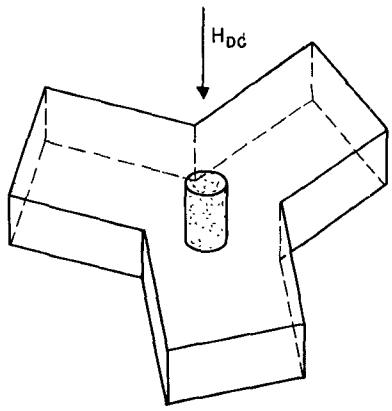

Fig. 16. Three-port H-plane waveguide circulator.

cylindrical axis of the post. With rectangular waveguide operating in the dominant TE_{10} mode, and with the ferrite post being considerably smaller in diameter than the width of the waveguide, the ferrite is excited mainly by the transverse RF H-field of the wave.

The operation of the waveguide circulator can be developed in a manner similar to that of the strip-line circulator [9]. First let us consider a lightly coupled case in which the ferrite post is contained in a cylindrical cavity which is coupled to the branching waveguides by small irises as shown in Fig. 17. If we assume this cavity is resonant at the operating frequency in the TM_{110} mode, the field pattern will be similar to that shown in the figure. Such a standing-wave pattern can be generated by two similar counter rotating patterns. The RF magnetic field will be almost circularly polarized in the ferrite for each sense of rotation. As soon as magnetic biasing field is applied to the ferrite, the resonance splits in a manner similar to that of the strip-line circulator. If the bias is adjusted so that each of the counter-rotating modes has a 30° phase angle, the resultant standing-wave pattern will have the orientation shown in Fig. 17. Here it is obvious that two ports are coupled to the standing-wave pattern and the third port lies at a null. This is equivalent to the $n=1$ mode circulation of the strip-line junction. Calculation of the frequency of resonance of this cavity is possible if small coupling is assumed. Writing down expressions for the fields in the ferrite and air portions, and equating E_z, B_r, and H_θ at the ferrite air boundary will yield an equation which could be solved for the resonant frequency. However, in the case of the actual circulator, the coupling irises are enlarged to the full size of the waveguide so that the cavity boundaries are no longer well defined. This is the equivalent of the broadbanding of the stripline circulator by tighter coupling to the feed lines. The calculation of the operating frequency becomes difficult in this case. Additional broadbanding can be obtained by impedance transforming means. One often used method is to make the circulator in reduced height, hence low-impedance waveguide, and to match to normal waveguide by stepped transformer

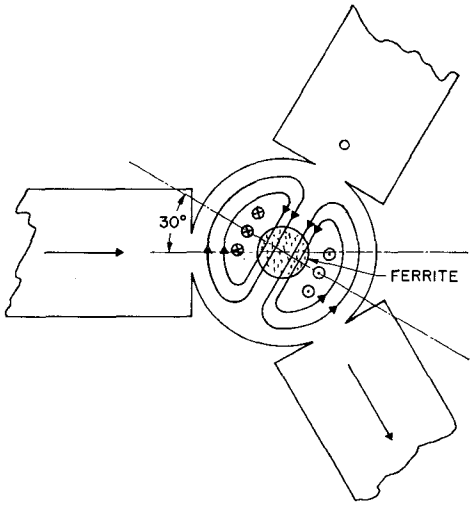

Fig. 17. Mode pattern for H-plane waveguide circulator using TM_{110} mode.

sections. Another method is to use triangular shaped ferrites whose points are in the centers of the waveguides. The points of the triangles are probably in regions of nearly linear polarization so that they are acting more like dielectric tapers than ferrimagnetic material. A partial height ferrite post compensated for by increased diameter also may be used, as well as a reduced diameter post with dielectric sleeve to maintain the proper resonant frequency.

The waveguide circulator can operate in the $n=2$ mode also in a manner similar to the strip-line case. However, the larger ferrite required, with its probable higher loss, makes this mode unattractive.

The E-Plane Y-Junction Waveguide Circulator

An E-plane waveguide Y-junction circulator can also be made [13]. The ferrite post in this case is mounted perpendicular to the narrow wall junction and is excited by the longitudinal RF H-fields. The cavity mode involved in this case is a TE_{111} mode as illustrated in Fig. 18. It is advantageous here to remove the center portion of the ferrite post leaving only two short cylinders at the ends of the cavity, since the center of the cavity is not active magnetically and ferrite here is of little value as well as a possible source of some loss. There is no strip line equivalent to this device since there are no longitudinal H-fields in TEM mode line.

The E-plane junction circulator has not been used to any extent. It might be advantageous in high power applications since the ferrite can be confined to regions of low E-field. It has some disadvantage in that a large air gap in the magnetic biasing circuit is inherent.

The Four-Port X-Junction Circulator in Waveguide

A few four-port waveguide junction circulators or X-junction circulators, have been described [14], [15]. These operate in a manner similar to the strip-line four-port junction. The TM_{110} cavity mode is operated with

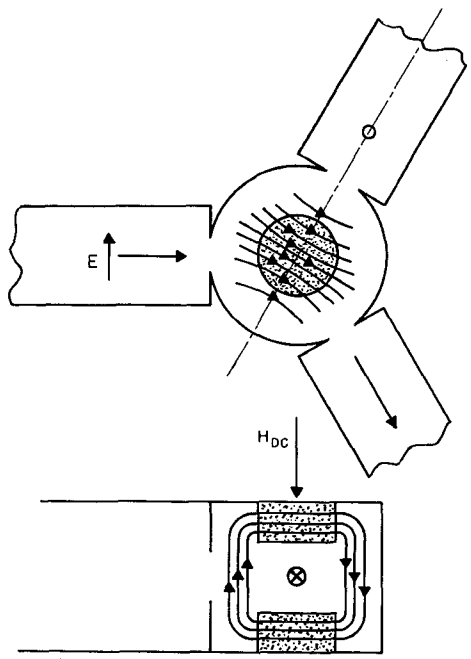

Fig. 18. E-plane waveguide circulator using TE_{111} mode.

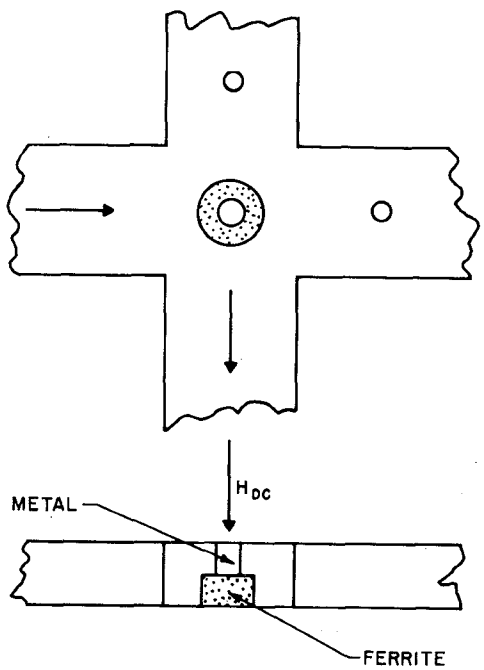

Fig. 19. Waveguide four-port circulator.

a 45° rotation of the standing-wave pattern and the TM_{010} cavity mode tuned to resonate at the same frequency by means of a central metallic post as illustrated in Fig. 19. The ferrite post and the metallic post are usually each partial height.

Conclusion

The operation of the ferrite junction circulator has been explained on the basis of a split resonance of the junction in which the standing-wave pattern of the

resonator is rotated to produce a null or no coupling at the isolated port. The derivation of the field relations necessary to provide the above condition for the strip-line case has been carried out and experimental verification of the normal modes of the resonator and the postulated field distribution for circulation have been shown. A design procedure using the quarter-wave transformer for matching a strip-line circulator has been outlined.

While the explanation and analysis of the strip-line circulator given here has been based on a circular disk and cylindrical ferrite structure for simplicity, it seems reasonable that the same basic principles should apply to other structures having a threefold symmetry. These principles are:

1) The symmetrical microwave circuit must support two counter-rotating modes which in the absence of a magnetic biasing field are degenerate.
2) The degeneracy must be removed by a magnetic biasing field directed along the axis of symmetry.
3) Circulation then will occur at a frequency between the resonant frequencies of the nondegenerate modes.
4) The splitting of the nondegenerate modes must be adjusted to approximate the desired bandwidth, which is determined by the degree of external coupling to the microwave circuit, (31).

The basic resonator can, in principle, extend well beyond the ferrite loaded portion, since the ferrite is useful only where the RF H fields approach circular polarization. Other symmetrical junctions which have been used are simple 120° strip-line junctions without a circular disk, and triangular junctions of both ferrite and center conductor. Application of these principles to waveguide circulators has been outlined.

Acknowledgment

The authors are indebted to L. K. Anderson and B. A. Auld for many constructive suggestions and criticisms.

References

[1] Fowler, H., presented at Symposium on Mircowave Properties and Applications of Ferrites, Harvard University, Cambridge, Mass., Apr, 1956.
[2] Schauge-Pettersen, T., Novel design of a 3-port circulator, Norwegian Defense Establishment Rept. 1958.
[3] Swanson, W. E., and G. J. Wheeler, Tee circulator, *IRE WESCON Conv. Rec.*, pt. 1, 1958, pp 151–156.
[4] Chait, H. N., and T. R. Curry, A new type *Y*-circulator, *J. Appl. Phys.*, suppl. vol 30, Apr 1959, pp 152S–153S.
[5] Auld, B. A., The synthesis of symmetrical waveguide circulators, *IRE Trans. on Microwave Theory and Techniques*, vol MTT-7, Apr 1959, pp 238–246.
[6] Milano, U., J. Saunders, and L. Davis, A *Y*-junction stripline circulator, *IRE Trans. on Microwave Theory and Techniques*, vol MTT-8, May 1960, pp 346–351.
[7] Bosma, H. On the principle of strip line circulation, *Proc. IEE*, vol 109, pt B, suppl 21, Jan 1962, pp 137–146.
[8] Bosma, H., On strip line *Y*-circulation at UHF, *IEEE Trans. on Microwave Theory and Technique*, vol MTT-12, Jan 1964, pp 61–72.
[9] Butterweck, H. J., Der *Y* Zirkulator, *AEU*, vol 17, Apr 1963, pp 163–176.
[10] Lax, B., and K. J. Button, *Microwave Ferrites and Ferrimagnetics*, New York: McGraw-Hill, 1962.
[11] Suhl, H., and L. R. Walker, Topics in guided wave propagation through gyromagnetic media, *Bell Sys. Tech. J.* vol 33, May 1954, pp 579–659; Jul 1954, pp 939–986; Sep 1964, pp 1133–1194.
[12] Editorial, *Microwaves*, vol 2, p 92, Aug 1963.
[13] Yoshida, S., *E*-Type T circulator, *Proc. IRE* (*Correspondence*), vol 47, Nov 1959, p. 2018.
[14] Yoshida, S., *X* circulator, *Proc. IRE* (*Correspondence*), vol 47, Jun 1959, p. 1150.
[15] Davis, L. E., M. D. Coleman, and J. J. Cotter, Four-port crossed waveguide junction circulators, *IEEE Trans. on Microwave Theory and Techniques*, vol MTT-12, Jan 1964, pp 43–47.